BEAM QUALITY STUDY IN RCNP SIX-SECTOR RING CYCLOTRON

T. Yamazaki, K. Hosono, Y. Misaki and I. Miura
Research Center for Nuclear Physics, Osaka University
Mihogaoka, Ibaraki, Osaka 567, Japan

Summary

Proposed ring cyclotron consists of six-sector magnets, three accelerating cavities and a flat-topping cavity. Assuming various voltage distributions in these cavities, beam behaviors have been calculated.

An unbalance of acceleration voltages generates the motion of the orbit center. The radial betatron amplitude grows by a perturbation relating to energy gain at cavities and a radial periodic field distribution, which is produced by the field correction using trim coils. This effect can be canceled completely by a rearrangement of cavity voltage and a first harmonic field component.

Theoretical results on perturbations by the radial periodic field predict the existence of a radial betatron resonance for cyclotrons with different numbers of sectors and cavities.

Introduction

An intermediate energy ring cyclotron to accelerate protons upto 400 MeV has been proposed at RCNP. The proposed accelerator system consists of two cyclotrons. The first one is an AVF cyclotron[1] which has been operating. The second one is a six-sector ring cyclotron[2] which has been designed to get high quality beams of protons and light ions for precise nuclear physics studies in high resolution.

The range of the acceleration frequency for the injector cyclotron is 6-18 MHz, and particles have been accelerated with the fundamental mode. The beam extraction radius of the injector cyclotron is 1m, and the beam injection radius of the ring cyclotron is 2m. The range of the acceleration frequency for the ring cyclotron is 30-50 MHz, and the particles are accelerated with the sixth and tenth harmonic RF modes.

Since the particles are accelerated with higher harmonic RF mode, a flat-topping cavity is used to get larger phase acceptance in the ring cyclotron. Because of spiral sector magnets, the acceleration gaps are tilted. Therefore it is necessary to investigate the relation between an orbit property of accelerated particles and the characteristics of cavities. This ring cyclotron uses only one flat-topping cavities, and an unbalance of cavity voltages will generate an effect equivalent to the first harmonic field perturbation.

Orbit Analyses

The orbit analyses have been done using isochronous field distributions. Injection and extraction radii of the ring cyclotron are 2.0m and 4.0m respectively. An equilibrium orbit of a particle is calculated at radius near 3.0m, and the particle is decelerated down to injection radius to determine the central ray of the injected beam. The injection and extraction systems are assumed to satisfy the central-position phase matching condition. Radial emittance of the injected beam was assumed to be 10mm•mrad in many cases. The orbit analyses were done for an ideal case in which the energy width of the injected beam is zero.

The field distributions of the sector magnets were generated by a computer code. The measured values with model magnet with a different shape were fitted by a analytical expression by the least square methods. The effective field boundary and the fringing field are parametrized.

The RF harmonic number is six and ten for protons and alpha particles, respectively. For the lower energy heavy ions twelfth harmonic acceleration is also applicable. Three acceleration cavities and a flat-topping cavity are used. A delta-shape dee with an angle of 18 degrees is assumed for the acceleration cavity. The positions of the acceleration gaps are 52° and 70° for the first cavity, 172° and 190° for the second cavity, and 292° and 310° for the third cavity. The position of the flat-topping cavity is 242°. These acceleration gaps are tilted to 5.164°.

Longitudinal Motion

The 18°-dee does not satisfy the peak acceleration condition for the sixth harmonic RF mode. However no remarkable radial-longitudinal coupling effect is seen in the phase ellipses. If proton beam with RF phase width 7° is accelerated to 400 MeV by sinusoidal acceleration voltage, the energy width of 700 keV is generated. This energy broadening can be canceled perfectly with a flat-topping cavity. If the phase errors between the cavities are less than 0.1 degree, the energy width of the 400 MeV protons is less than 10^{-4}.

The ratio of the acceleration voltage at extraction to injection radii (V_{ext}/V_{inj}) should not be much larger than one. At the extraction radius the energy width of the injected beam will be multiplied by this ratio. Consequently, large phase compression of beam can not be expected.

The wide phase acceptance for single turn extraction mode with a flat-topping is desirable to get high intensity beam. The phase acceptance depends much for the radial distribution of the acceleration voltage as shown in Fig. 1. Phase acceptance of 20° width can be expected for flat voltage distribution (Fig. 1a). In Figs. 1b and 1c the convex distribution is assumed for the flat-topping cavity. In case of the concave distribution for the acceleration cavities, the beam phase width expands as the dee voltages decrease in mid course of the acceleration and the beam energy gain is small for early and late phases. At the extraction radius the dee voltage recoveries to that at injection radius, and the beam phase width compresses to original value. The concave distribution has a narrower phase acceptance. In the case of convex distribution for the acceleration cavities, the beam phase width compresses as the dee voltages increase in mid course of the acceleration and the beams with wider phase width at the injection can be accelerated within the flat-topping region of the acceleration phase but with larger energy width at each phase. At the extraction radius the dee voltage decreases to that at injection radius and beam phase width expands with the recovery of energy width at each phase. As a result a wide phase acceptance can be realized by the convex distribution as shown in Fig. 1.

Because of spiral magnets acceleration cavities are tilt. The calculations of the accelerated orbits usualy use tilt angle of 5.164 degrees for all cavities. In mid course of the acceleration the energy width of beam becomes larger, and the RF phase of the flat-topping cavity is adjusted so as to minimize the energy width at the extraction radius. The particles accelerated with different phases have almost the same radii for the same turns at an angle calculated, and it is expected to get well separated turns on the measurements by a radial differential probe. If the tilt angle of the flat-topping cavity is changed to 4.924 degrees and other dee cavities are set to 5.164 degrees we can get both small energy width and radial width in mid course of the acceleration and also at the extraction radius.

Radial Motion

Protons are accelerated through $\nu_r = 6/5$ resonance. The 400 MeV protons cross $\nu_r = 6/4$ resonance at radius near extraction. As expected from its order, the effect of $\nu_r = 6/5$ resonance is relatively small. The radial phase ellipse of the accelerated proton beam was traced from the injection radius to the extraction radius, but no remarkable deformation of the phase ellipses is observed in numerical calculation. A radial oscillation of corrected magnetic field produced by using trim coils is simulated by the superposition of a periodic field component with a constant amplitude and a constant period. This field modulates the betatron frequencies ν_r and ν_z. Figure 2 shows a radial phase plot of 207 MeV proton acceleration with the radial periodic field. Figure 2a is the phase plot covering a large amplitude oscillation. A stable region is quite large, and the fixed points of $\nu_r = 6/5$ resonance and separatrix lines are located 40cm apart from the equlibrium orbit. Figure 2b expands the center region of Fig. 2a. Here, five islands and corresonding fixed points of $\nu_r = 6/5$ resonance appear again at only 1cm apart from the equilibrium orbit. The fixed points outside the stable region appear from the global characteristics of the field distribution, and move slowly with particle energy on the phase plot. The fixed points around the equilibrium orbit appear from the local rapid variation of the field, and move around the equilibrium orbit.

Introducing a flat-topping cavity increases the amplitude of radial betatron oscillation, but this growth is suppressed by a rearrangement of the cavity voltages and an adjustment of the first harmonic field. This procedure is discussed in the following section.

Radial Periodic Field and Resonances

Effect of Flat-topping Cavity

Many trim coils are used to adjust the radial profile of the magnetic field. To minimize the difference between the ideal isochronous field and the corrected field with trim coils, it is desirable to increase the number of trim coils as many as possible. This corrected field was simulated by adding a radial periodic field with an equal period and the same amplitude. The accelerated orbits of 207 MeV protons were calculated with a field including the radial sinusoidal component of 3 gauss amplitude and 45 mm radial periodicity.

Starting from an accelerated equilibrium orbit at some radius, particle was traced forward and backward to get accelerated orbit. When a radial increase in $1/(\nu_r-1)$ revolutions coincides with the period of radial sinusoidal field, a computer result shows a growth of radial oscillation. The radial position of this resonance depends on the acceleration voltage. Higher voltage shifts the position of resonance to larger radius.

After seven to ten periods of the radial betatron oscillation a growth of resonance amplitude stops. The final amplitude depends on the voltage of flat-topping cavity, and the resonance disappears without flat-topping cavity or by using two flat-topping cavities that confronts each other. By introducing force to shift an orbit center with the first harmonic field perturbation or to put different voltages to three delta-type cavities, the accelerated particles cross the resonance. This fact suggests a method to compensate the resonance by adjusting the accelerating voltage of cavities or generating the first harmonic field by using harmonic coils.

Theory

The electric gap-crossing resonance[3] and the bevelled dee effect in an AVF cyclotron[4] produce an equivalent first harmonic field perturbation, and the orbit center oscillates with a frequency ν_r-1 around the cyclotron center. In the gap-crossing resonance the difference between the number of sector magnets and the number of equally spaced acceleration gaps is one, the perturbations produced by this structure have Fourier components in resonance with ν_r. In the case of a bevelled dee the displacement of orbit center at a dee gap is not canceled in the next passage, and the orbit center undergoes a displacement at every turn.

If only one flat-topping cavity is used in a ring cyclotron, the orbit center displacement is occurred like the bevelled dee. When the particle accelerates with a frequency ν_r-1 in radial periodic field in addition to the main isochronous field, the perturbations produced by the crossing of the flat-topping gap and radial periodic field Fourier components will have a frequency ν_r. For an evaluation of this effect similar procedure as the gap crossing resonance[3] can be used.

The instantaneous equilibrium orbit

$$r_e(p,\theta) = R[1+\xi(R,\theta)]$$

is chosen as a reference orbit, where R is the average radius and ξ has zero average value. An accelerated orbit is given by

$$r(\theta) = r_e(p,\theta) + x(\theta),$$

where $x(\theta)$ is the displacement of the orbit from the reference orbit, and assume that the amplitude of $x(\theta)$ is smaller than the period of radial periodic field component. The coordinate $x(\theta)$ is transformed to a coordinate $X(\theta)$. An independent variable ϕ and a coordinate $y = y(\phi)$ is introduced by

$$X(\theta) = W(\theta)y(\phi),\ \phi = \theta+\psi \text{ and } W^2(1+\dot{\psi}) = 1.$$

The differential equation for $y(\phi)$ is

$$d^2y(\phi)/d\phi^2 + \nu_r{}^2 y(\phi) = F(y,\phi),$$

where $F(y,\phi)$ is the force associated with the magnetic field $B(r,\theta)$ and the momentum change p at each gap. This force involves the quantity λ defined by

$$\lambda(\theta) = \dot{R}/R,$$

where dot denotes derivative with respect to θ. At each gap-crossing λ changes discontinuously. A gap geometry is assumed as follows. There are N_c gap-crossings at $\theta = 2\pi/N_c$ and the same delta-function type energy gain at each gap-crossing, and a flat-topping gap is located at θ_f. The value of $\lambda(\theta)$ is expanded to

$$\lambda(\theta) = \lambda_0(1+2\sum_{n=1}^{\infty}\cos nN_c\theta) + \delta\lambda_0(1+2\sum_{n=1}^{\infty}\cos n(\theta-\theta_f)).$$

The perturbation relating to radial periodic field becomes

$$\begin{aligned} F(y,\phi) = &-(pR)^{1/2}[k_0+((3/2)k_0+k_1)\xi \\ &+3k_0w+(3/2)\lambda k_0\xi_\theta] \\ &-y(\phi)[k_0+k_1+(k_0+3k_1+k_2)\xi \\ &+3\lambda(k_0+k_1)\xi_\theta], \end{aligned}$$

where terms of higher than first-order in ξ, w and λ and terms of second and higher order terms in $y(\theta)$ have been neglected. The quantities ξ_θ, w, k_0, k_1 and k_2 are defined by

$$\xi_\theta = \partial\xi/\partial\theta, \qquad W(\theta) = 1+w(\theta),$$

$$k_0 = B_T/B_0,\ k_1 = \frac{R}{B_0}\frac{dB_T}{dR} \text{ and } k_2 = \frac{R^2}{B_0}\frac{d^2B_T}{dR^2}.$$

The quantity $B_0(R)$ is isochronous field, $B_T(R,\theta)$ is radial periodic field including azimuthal dependence. The magnetic field is defined by

$$B(r,\theta) = B_0(r)(1+\sum_n b_n \cos n(\theta-\theta_n)) + B_T(r,\theta)$$

$$B_T(r,\theta) = b_t(r)(1+\sum_n B_{tn}(r,\theta))$$

$$b_t(r) = c \cos(2\pi r/d+\delta)$$

$$B_{tn}(r,\theta) = b_n(r)\cos n(\theta-\theta_n),$$

where c and d are amplitude and period of radial field, respectively. When a radial increase in $1/(\nu_r-1)$ revolutions coincides with the period of radial sinusoidal field d, the radial dependence of the field B_T can be expanded as

$$b_t(r) = \sum_{n=1}^{\infty} C_n \cos n((\nu_r-1)\theta+B_n).$$

Perturbation Effect

The rate of energy gain for the particle by delta-function type gap-crossing at $\theta=\theta_i$ is expressed as

$$\dot{E}_i(\theta) = (E_i/2\pi)(1+2\sum_{n=1}^{\infty}\cos n(\theta-\theta_i)).$$

The particle energy at angle θ is evaluated by

$$E(\theta) = \int_0^\theta (\sum_{i=1}^{N}\dot{E}_i(\theta))d\theta$$
$$= E_I+(E_1/2\pi)\theta+E_1\sum_{n=1}^{\infty}(e_n/n\pi)\sin n(\theta-\theta_n'),$$

where N is the number of cavities, E_I is the initial energy and E_1 is the energy gain in one turn. The factor $(pR)^{1/2}$ in the perturbation $F(y,\phi)$ is given by

$$f(\phi) = (pR)^{1/2}$$
$$= f_F(\phi)(1+(E_1/2E_F(\phi))\sum_{n=1}^{\infty}(e_n/n\pi)\sin n(\phi-\phi_n)),$$

where $E_F(\phi) = E_I+(E_1/2\pi)\phi$
and $f_F(\phi) \cong (2E_F(\phi)/eB_0)^{1/2}$.
The particle energy $E_F(\phi)$ and $f_F(\phi)$ are monotonic functions of angle ϕ.

(1) Single Flat-topping Gap and First Harmonic Field.

In the case of N_c gap-crossings at the same angular interval and the same energy gain at each gap-crossing, $f(\theta)$ has only $n=mN_c$ Fourier components. However, in the case of single flat-topping gap $f(\theta)$ has all Fourier components on n values. The first term of $F(y,\phi)$ is reduced to

$$F_1(\phi) = -(pR)^{1/2}k_0$$
$$= -(pR)^{1/2}\, b_t(R)(1+b_1(R)\cos(\theta-\theta_1)+\cdots)/B_0(R).$$

Now consider the case that the radial increase in $1/(\nu_r-1)$ revolutions is equal to the period of radial sinusoidal field. Since b_t has strong $n=\nu_r-1$ Fourier component and $(pR)^{1/2}$ has predominantly $n=1$ component for single flat-topping cavity, then $F_1(\phi)$ will have an $n=\nu_r$ component. If the first harmonic component is present in the magnetic field, from this component and strong $n=\nu_r-1$ component of radial sinusoidal field the perturbation $F_1(\phi)$ will have an $n=\nu_r$ component. The force in the presence of the flat-topping cavity is proportional to $E_1/2E_F$, where E_1/E_F is the ratio of the energy gain per turn to the particle energy. The force in the presence of the first harmonic field is proportional to $b_1(R)$ in cyclotron unit, i.e., the value $b_1(R)$ is the ratio of the strength of the first harmonic field to the average field. Since the other factors are common to two forces, it is possible to cancel these forces by selecting the voltage of flat-topping cavity and the strength and phase of the first harmonic field. Another method to suppress the force $F_1(\phi)$ is to eliminate the periodic parts of $f(\phi)$ by choosing suitable voltages of cavities. The computer results on the six sector cyclotron are shown in Fig. 3. The amplitude growth by this resonance is 5mm to 1cm, and this is comparable to the turn separations at larger radius. Therefore it is necessary to eliminate this effect. The figures also show that the cancelations are possible.

(2) Gap-crossing Resonance. The perturbation $F(\phi)$ has gap-crossing resonance terms:

$$F_2(\phi) = -(pR)^{1/2}(3/2)\lambda k_0\xi_\theta$$
$$-3\lambda(k_0+k_1)\xi_\theta y(\phi).$$

In the case of the so-called gap-crossing resonance[3] the perturbation has a term $F_G(\phi) = -(pR)^{1/2}\lambda(2+k)\xi_\theta$, where k is the field index, but it does not have a radial periodic field. Even if a radial periodic field is added in the perturbation, similar resonance condition as that of the gap-crossing resonance holds.

To evaluate the effect of this resonance, consider a unreal six sector cyclotron with five or seven gap-crossings at the same angular interval and the same energy gain at each gap-crossing. The field distribution for 207 MeV proton is used in the calculation. The value λ has strong n=5 and n=7 Fourier components for five and seven gap-crossings, respectively. Moreover, since ξ_θ has predominantly an n=6 component and the radial field k_0 has strong $n=\nu_r-1$ component, then the first term of $F_2(\phi)$ will have an n=1 component.

The radial field k_0 also has a weak $n=2(\nu_r-1)$ Fourier component. The value λ has n=10 and n=14 Fourier components for five and seven gap-crossings, respectively. Since ξ_θ has an n=12 component and function $y(\phi)$ has $n=\nu_r$ component, then the second term of $F_2(\phi)$ will have an n=1 component.

Figure 4 shows some computer results of the gap-crossing resonance including a radial periodic field. There are two resonances during particle acceleration as expected from the above discussion. The resonances occur at radii where the radial increases in $1/(\nu_r-1)$ and $2/(\nu_r-1)$ revolutions are equal to the period of radial sinusoidal field. Similar gap-crossing is also observed in computer calculations on four sector cyclotron with three or five cavities.

Since in the gap-crossing of the flat-topping cavity λ also has not only n=1 Fourier component but also n=5 and n=7 components, both the first and the second terms of the perturbation $F_2(\phi)$ have an n=1 component in a cyclotron with single flat-topping cavity.

For the six sector cyclotron the force by a single flat-topping gap (energy gain by this gap/turn=-56 kV) and the force by gap-crossing resonance of five accelerating gaps (energy gain by five gaps/turn=450 kV) will be compared. It is assumed that the particle energy is 100 MeV, and the amplitude of the equilibrium orbit ξ is 0.04. The force by a flat-topping gap is proportional to $E_1/2E_F = 0.00028$. Since the amplitude of ξ is 0.04, the amplitude of ξ_θ is 0.04×N, where N is the number of sectors. The amplitude of Nth component in λ is evaluated to

$$\lambda_N = E_N/(2\pi E_F(1+k)) = 0.00072$$

for five accelerating gaps, where k is the field index, and E_N is the energy gain by N gaps per turn. The $\lambda_5\xi_\theta$ value for five accelerating gaps is $\lambda_5\xi_0 = 0.00014$. By using these values the ratio of the force by a flat-topping gap to that by five accelerating gap becomes to 2, and is equal to the ratio of amplitude growths of radial betatron oscillation. The amplitude growth by the gap-crossing resonance in six sector cyclotron with seven cavities is very small, and is not interpreted by the force $F_2(\phi)$.

Axial Motion

To investigate the size of the stable region in the axial motion of particles static phase plot in the (z,p_z) plane was used. The radial component (r,p_r) of the starting point was chosen on an equilibrium orbit, and either of p_z or z component sets to non-zero value. In some case (r,p_r) values of traced particles shift from the equilibrium value after many revolutions, the projected (z,p_z) phase plots do not lie on a sharp line but fill a narrow band region. Especially these deviations are large for the plots within isolated islands in both (r,p_r) and (z,p_z) planes. This tendency is remarkable when the starting points of (r,p_r) values are set far from the equilibrium orbit.

The axial betatron frequency for the acceleration of 400 MeV protons always lie near $\nu_z = 6/6$ resonance. The phase plots near the extraction region is shown in Fig. 5a. A numerical study uses magnetic field values expanded in powers of z. If in the magnetic field the terms of higher than first order in z are neglected, axial phase plot does not show $\nu_z = 6/6$ resonance. If z^2 terms is added in the magnetic field, axial phase plot seems to indicate the existence of the resonance. If terms up to sixth order in z are added in the magnetic field, axial phase plot shows six islands related to $\nu_z = 6/6$ resonance. The figure shows a small stability region of height less than 2cm. If two magnets that confronts each other are set 1mm up and down by misalignment, the axial oscillation amplitude of 400 MeV protons exceeds 15mm (Fig. 6). Therefore, it is necessary to install magnets within 0.1 mm. Although particle does not cross the resonance, the axial growth is generated. The particles except high energy protons cross $\nu_z = 6/5$ resonance and heavy ions are accelerated up to $\nu_z = 6/4$ resonance region. The axial phase plot of $^{20}Ne^{5+}$ ions shows clearly the existence of $\nu_z = 6/4$ resonance as shown in Fig. 5b. By introducing two sector magnet misalignments the phase plot can indicate the fixed points and islands of $\nu_z = 6/5$ resonance. These resonances are weak, and no axial growth is seen in an accelerated orbit calculation.

The 207 MeV protons are accelerated along the coupled resonance $\nu_r = \nu_z$ (and $2\nu_r = 2\nu_z$), but the accelerated orbit studies with the displacement of (r,p_r,z,p_z) values from an equilibrium orbit give no indication of this coupled resonance.

References

1. M. Kondo, I. Miura, T. Yamazaki, H. Ejiri, A. Shimizu, M. Inoue, K. Hosono, T. Saito, Y. Nagai, H. Sakai, N. Matsuoka and S. Yamabe, Proc. 7th Int. Conf. on Cyc. and their Appl., Zurich (1975), p.95.; T. Itahashi et al., This Conf. H18.
2. I. Miura, T. Yamazaki, A. Shimizu, K. Hosono, T. Itahashi, T. Saito, A. Ando, K. Katayama, Y. Misaki and M. Kondo, This Conf. H20.
3. M.M. Gordon, NIM 18, 19 (1962) 201.
4. C.J.A. Corsten, W.M. Schulte and H.L. Hagedoorn, NIM 171 (1980) 1.

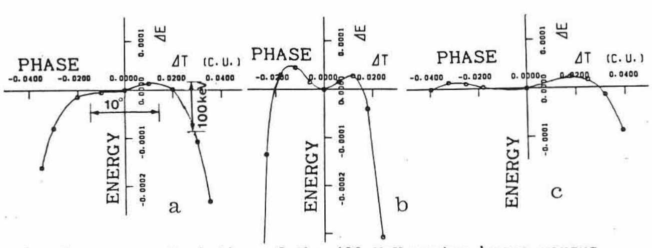

Fig. 1. Energy deviation of the 400 MeV proton beams versus acceleration phases for various radial voltage distributions.
a) flat distribution b) concave distribution
c) convex distribution

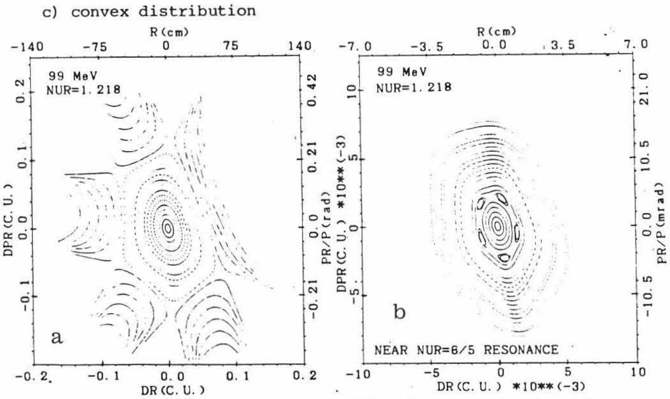

Fig. 2. Radial phase plot of 207 MeV proton acceleration. The magnetic field is assumed to include radial sinusoidal field with amplitude 3 Gauss and period 4.5 cm.

Fig. 3. The orbit motions of the 207 MeV protons in a six sector cyclotron with three dee cavities and a flat-topping cavity are shown by the radial displacement from the equilibrium orbit at 0°.
V_i = the voltage of dee cavity No. i (i = 1, 2 and 3)
V_f = the voltage of flat-topping cavity
a) $V_1=V_2=V_3$=125 kV, V_f= 0 kV. There is no resonance.
b) $V_1=V_2=V_3$=125 kV, V_f=-66.2 kV. The resonance appears by a flat-topping gap crossing.
c) $V_1=V_2=V_3$=250 kV, V_f=-132.5 kV. The resonance shifts to larger radius.
d) V_1=190 kV, $V_2=V_3$=280 kV, V_f=-132.5 kV. The resonance effect is cancelled by a rearrangement of cavity voltages.
e) $V_1=V_2=V_3$=250 kV, V_f=-132.5 kV. The resonance effect is cancelled by the first harmonic field. The magnetic fields of two sector magnets that confronts each other are changed $\pm$0.025 %.
f) The oscillation of radial betatron frequency ν_r shows the periodicity of radial sinusoidal field.

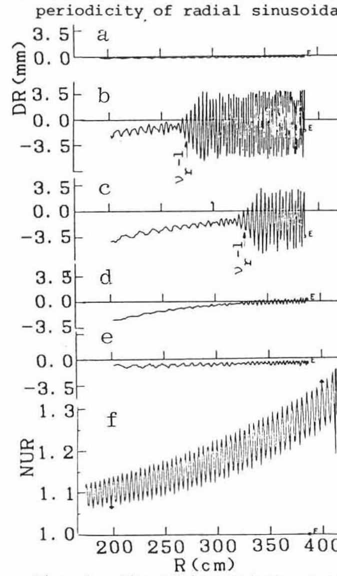

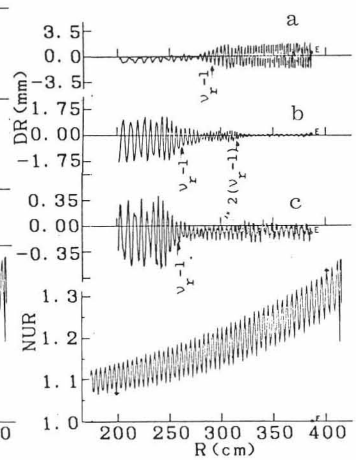

Fig. 4. The orbit motions of the 207 MeV protons in a six sector cyclotron with five and seven cavities are shown by the radial displacement from the equilibrium orbit at 0°.
a) five cavities, V=125 kV. The gap crossing resonance.
b) five cavities, V=90 kV. The proton is decelerated from larger radius. There are two gap-crossing resonances.
c) seven cavities, V=60 kV. The proton is decelerated from larger radius. The effect of gap-crossing resonance is small.

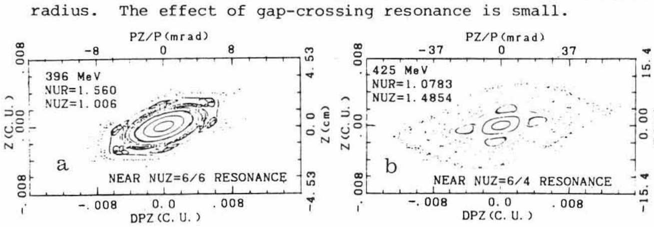

Fig. 5. Axial phase plots.
a) plot of the 400 MeV protons near ν_z=6/6 resonance.
b) plot of the 425 MeV Neon-20(5+) ions near ν_z=6/4 resonance.

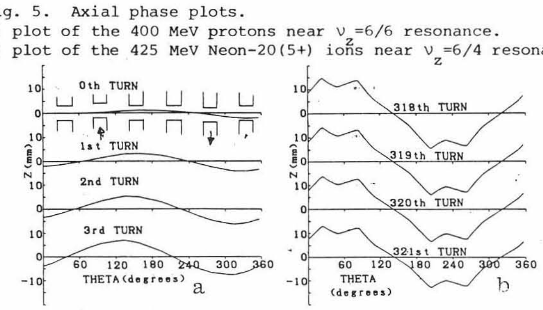

Fig. 6. Axial oscillation of the 400 MeV protons. Two magnets that confronts each other are set 1 mm up and down by misalignment.
a) initial four turns b) last four turns